Steel and Composite Structures, *Vol. 19, No. 5 (2015) 1145-1165*
DOI: http://dx.doi.org/10.12989/scs.2015.19.5.1145

Analytical investigation of thin steel plate shear walls with screwed infill plate

Cüneyt Vatansever [*1] and Jeffrey W. Berman [2a]

[1] *Department of Civil Engineering, Faculty of Civil Engineering, Istanbul Technical University, Istanbul, Turkey*
[2] *Department of Civil and Environmental Engineering, University of Washington, Seattle, WA, USA*

(*Received November 03, 2014, Revised April 20, 2015, Accepted April 25, 2015*)

Abstract. A behavior model for screw connections is developed to provide a better representation of the nonlinear response of thin steel plate shear walls (TSPSWs) with infill plates attached to the boundary frame members via self-drilling screws. This analytical representation is based on the load-bearing deformation relationship between the infill plate and the screw threads. The model can be easily implemented in strip models of TSPSWs where the tension field action of the infill plates is represented by a series of parallel discrete tension-only strips. Previously reported experimental results from tests of two different TSPSWs are used to provide experimental validation of the modeling approach. The beam-to-column connection behavior was also included in the analyses using a four parameter rotational spring model that was calibrated to a test of an identical frame as used for the TSPSW specimens but without the infill plates. The complete TSPSW models consisting of strips representing the infill plates, zero length elements representing the load-bearing deformation response of the screw connection at each end of the strips and the four parameter spring model at each beam-to-column connection are shown to have good agreement with the experimental results. The resulting models should enable design and analysis of TSPSWs for both new construction and retrofit of existing buildings.

Keywords: screw connection; steel plate shear wall; strip model; tension field action; bearing deformation

1. Introduction

Steel plate shear walls (SPSWs) with unstiffened infill plates that resist loads primarily through the development of post-buckling tension field action have been found to be effective seismic and wind load resisting systems for buildings as they have high strength, stiffness, and ductility (Timler and Kulak 1983, Caccese *et al*. 1993, Driver *et al*. 1998b, Lubel *et al*. 2000, Berman and Bruneau 2005, Chen and Jhang 2006, Choi and Park 2009, Jahanpour *et al*. 2012). Guo *et al*. (2012) also showed that both SPSW and composite SPSW systems achieved good ductility and energy dissipation capacity. These systems may also be useful for retrofitting existing steel buildings. The use of SPSWs with relatively thick hot-rolled infill plates (typically greater than 3

∗Corresponding author, Assistant Professor, E-mail: cuneyt.vatansever@itu.edu.tr
[a] Associate Professor, E-mail: jwberman@u.washington.edu

http://www.techno-press.org/?journal=scs&subpage=8 ISSN: 1229-9367 (Print), 1598-6233 (Online)

mm thickness) in seismic retrofit situations, where they would be installed in an existing bay, would likely require reinforcement of the existing beams and columns due to the large moments induced from the plate yielding in tension field action. However, the use of thinner, possibly cold-rolled, infill plates may not require the existing frame members be strengthened, minimizing retrofit costs despite requiring the use of multiple bays of infill plates. Kurata *et al*. (2012) also demonstrated that the rehabilitation of a steel frame with SPSW using relatively thin infill plate and having supplemental elements as tension-bracing achieved stable hysteretic behavior. An additional advantage of using thinner plates is that they can easily be installed and removed to accommodate renovations if screw connections are used. Further retrofit advantages may be found if thin infill plates can be used effectively in bays that do not have fully restrained beam-to-column connections.

Steel plate shear walls have typically been designed for seismic applications with infill plates that are connected to the boundary frames via welds or bolts. A critical issue in SPSW seismic design is to ensure that the infill plates can develop tension field yielding before the beams and columns reach their capacity or failure of the infill plate-to-boundary frame connection occurs. After significant infill plate yielding, the infill plate-to-boundary frame connection may acceptably begin to degrade as long as the failure mode for the connection is slow tearing or bearing failure of the infill plates around fasteners or adjacent to welds. The connection is long enough that small tears may take several cycles before propagating to be large enough to cause strength degradation, whereas shearing of fasteners themselves is likely to be brittle and should be avoided. As a result screwed and bolted connections are the most suitable system for very thin steel cold-formed panels where ductility is critical (Matteis and Landolfo 1999).

SPSW behavior is significantly affected by the infill plate-to-boundary connection. Elgaaly and Liu (1997) noted that SPSWs with bolted infill plate connections have smaller elastic stiffness and lower initial yield load. Therefore, they developed an analytical model for representing the infill plate considering both welded and bolted connections between the infill plates and the boundary frame members. The connection deformation was incorporated into the behavior of the individual strips in the strip model representation of SPSWs, where the infill plate tension field action is represented by a series of discreet tension-only pin-ended elements inclined at the angle of inclination of the tension field as originally proposed by Thorburn *et al*. (1983) and modified by others as discussed in Sabelli and Bruneau (2007). Kharrazi *et al*. (2011) has also proposed a model and demonstrated the implementation of it (Kharrazi *et al*. 2008) which is called Modified Plate-Frame Interaction (M-PFI) to eliminate the inadequacy of PFI model which was originally presented by Sabouri-Ghomi *et al*. (2005). A new method to assess the ultimate shear capacity of the semi-supported steel shear walls has been presented by Jahanpour *et al*. (2011). The behavioral differences under cyclic loading between SPSWs with welded and bolted infill plate connections in terms of deformation capacity and energy dissipation have also been reported in Choi and Park (2009).

Vatansever and Yardımcı (2011) united the concepts of SPSWs with thin cold-formed infill plates (TSPSWs) that are easily installed with screw connections to the boundary frame members. That research included testing of two different TSPSWs under quasi-static cyclic loading to large inelastic deformations and similar testing of the bare boundary frame. The main objective of this study is to analyze and interpret the effect of the infill plate screw connection to boundary frame members on overall TSPSW response. Here, the development of a behavior model for the screw connections is described to provide a better representation of the response of TSPSWs with infill plates attached to the boundary frame members via screws. This analytical representation is based

on the load-bearing deformation relationship between the infill plate and the screw threads under monotonic loading. The screw model is then incorporated into strip models of the two TSPSWs tested by Vatansever (2008). The experimental and analytical results are compared for the entire range of hysteretic TSPSW response and resulting suitable numerical models for the screw connections are recommended.

2. Test specimens and setup

Two TSPSWs, denoted SW-A-H and SW-B-H, were tested under cyclic loading and are shown in Figs.1 and 2, respectively. As shown, the infill plate of Specimen SW-A-H was connected to boundary frame members on all four sides while the infill plate of Specimen SW-B-H was connected only to the beams of the boundary frame. Additionally, a bare frame specimen, denoted BF-H, which had identical boundary frame members and beam-to-column connections as the TSPSW specimens, was tested to document the behavior of the system without the infill plates and to provide data for the development of an analytical model that includes the beam-to-column connection behavior. The specimens were designed at 1/3 scale due to actuator force limitations and space restrictions. Specimen design, details, and experimental results are only briefly reviewed here and additional details may be found in Vatansever and Yardımcı (2011).

Figs. 1 and 2 show the overall specimen dimensions, the infill plate thicknesses, t, and the boundary frame members' sizes in their Eurocode standard designations. The boundary frame members and 6.0mm thick fish plates were designed to remain elastic so that they could be reused for additional tests. The beam-to-column connections were header plate connections where end plates were welded to the beam web and bolted to the column flanges by M16-10.9 bolts. Fig. 3 shows a schematic of the experimental setup. Lateral bracing was also provided to the specimen through the use of steel rollers that were set to roll at mid-depth of the web of the specimen's upper beam. Each specimen was subjected to a quasi-static loading protocol with displacement applied in increasing amplitude cycles consistent with ATC 24 (Applied Technology Council 1992).

Tension tests of the infill plate materials were performed. The elastic modulii, yield stresses

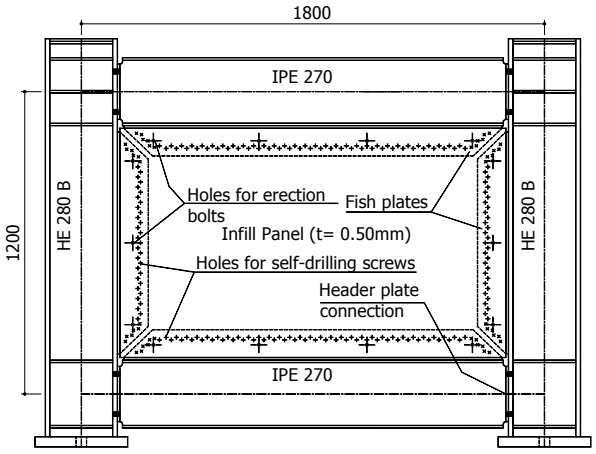

Fig. 1 Details of specimen SW-A-H (Dimensions in mm)

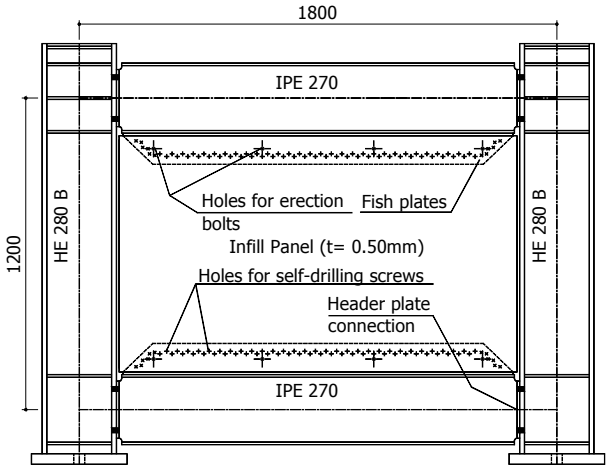

Fig. 2 Details of specimen SW-B-H (Dimensions in mm)

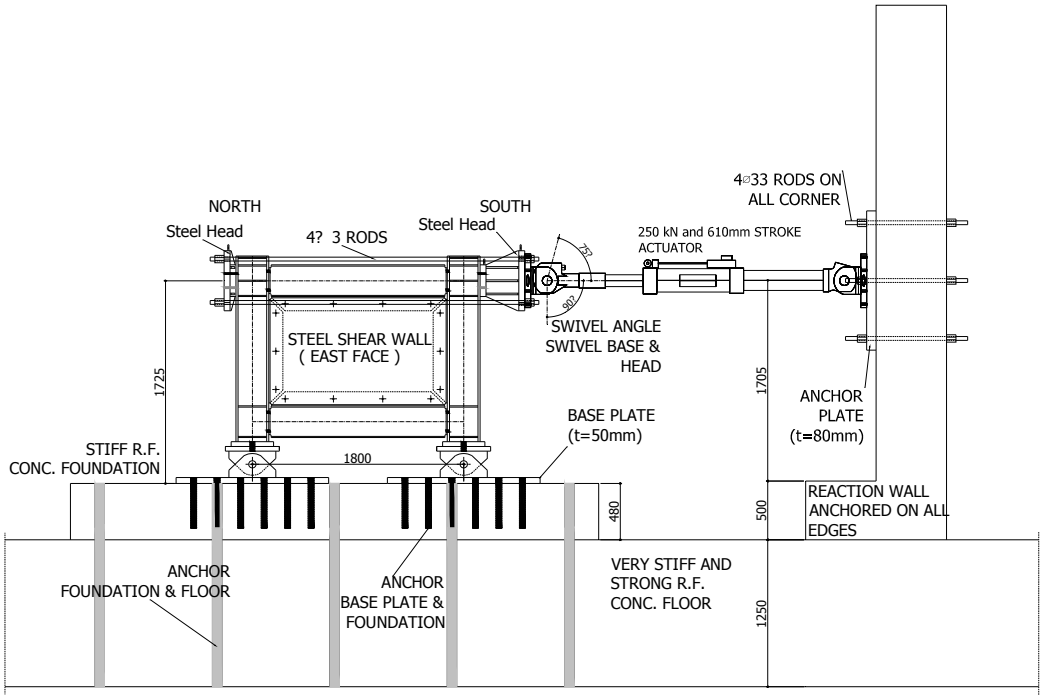

Fig. 3 Test setup (Dimensions in mm)

and ultimate stresses of the infill plates of SW-A-H and SW-B-H were 198515 MPa and 194623 MPa, 198.5 MPa and 179.5 MPa, and 333.5 MPa and 311.9 MPa, respectively. The material of the boundary frames and fish plates was specified to be S275 (yield stress, 275 MPa) and S235 (yield stress, 235 MPa), respectively, which European steel grades. Tension tests were not performed on that material because the boundary members remained elastic during the tests.

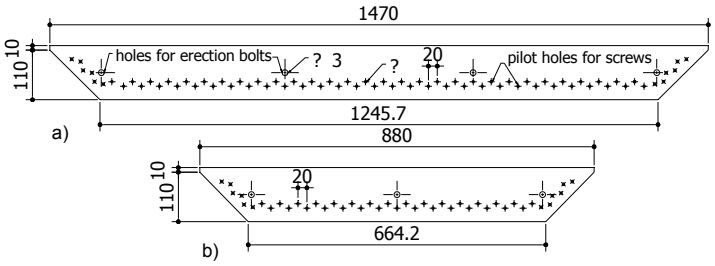

Fig. 4 Details of fish plates connected to: (a) beams; and (b) columns (Dimensions in mm)

3. Infill plate-to-boundary frame screw connection design

The primary design objective for the connection of infill plate to the boundary frame is that it be able to develop the full tension field strength of the infill plates under repeated cyclic loading. Therefore, the connections have an important role in ensuring ductile system behavior. In general, the type and arrangement of fasteners have a fundamental influence on strength, stiffness, deformation capacity and energy dissipation of TSPSW systems. Here, the infill plate thickness of 0.50 mm prohibited the use of welds or large diameter high strength bolts for the connection and instead required the use of unconventional fasteners for attaching them to the boundary frame. Self-drilling screws with a nominal diameter of 5.50 mm were selected as the best means of connecting the infill plates to the fish plates. Such screws allow for rapid installation of the infill plates in retrofit situations and, as shown below, also provide for adequate TSPSW performance.

The number of screws required was calculated to ensure full development of tension field yielding of the infill plates and considering infill plate strain hardening of 10%. The limit state of bearing strength controlled the screw connection design. Two screw lines were used with a 10 mm distance between them to accommodate the required number of screws. To prevent net section fracture of the infill plates prior to achieving yield, a minimum distance between two adjacent screws of three times the diameter of the screw was used. To best achieve this spacing, the holes in the two lines were staggered. A limited number of erection bolts were also included to help in properly installing the infill plates. Details of the infill plate-to-fish plate connections are shown in Fig. 4 and were the same for both TSPSW specimens except that SW-B-H had only the connection to the beams.

4. Design and modeling of beam-to-column connection

The beam-to-column joints were designed as header plate connections using end plates which were welded only to the beam web and bolted to the column flanges by M16-10.9 bolts. More detail can be found in Vatansever and Yardımcı (2011).

Since the beams and columns were designed to remain elastic, the boundary frame's inelastic behavior is characterized by the moment-rotation behavior of the beam-to-column connections rather than the contribution of the relatively rigid beams and columns. Therefore, the moment-rotation relationship for the header plate connection is required. The four parameter nonlinear representation of the moment-rotation curve expressed by Eq. (1) was used (Goldberg and Richard 1963, Abbott and Richard 1975) to model the nonlinear behavior of header plate beam-to-column connections.

$$M = \frac{(K_\phi - K_{\phi,p}) \times \phi}{\left(1 + \left|\frac{(K_\phi - K_{\phi,p}) \times \phi}{M_o}\right|^n\right)^{1/n}} + K_{\phi,p} \times \phi \tag{1}$$

K_φ is the initial stiffness,
$K_{\varphi,p}$ is the plastic stiffness,
M_o is the reference moment,
M is the computed moment,
n is the shape factor,
φ is the rotation.

To apply Eq. (1) and develop the moment-rotation curve of a beam-to-column joint, the initial and plastic stiffnesses and the reference bending moment of the connection must be calculated. In addition, a reasonable range of rotation values should be used. Here, the initial stiffness, K_φ and reference bending moment, M_o, were initially obtained based on the provisions of Eurocode 3 (EC3) (European Convention for Constructional Steelwork 2005). The parameters $K_{\varphi,p}$ and n were found by calibrating the bare frame model with the test results for BF-H. These properties were then used in subsequent analyses of the strip models described below. The connection model parameters were calibrated over connection rotations from 0.00 rad to 0.026 rad (Vatansever and Yardımcı 2011). The resulting moment-rotation curve is given in Fig. 5.

As described below, the structural analysis program OpenSEES (Mazzoni *et al*. 2009) was used for analysis of the TSPSW specimens. In OpenSEES the Hysteretic Material, which is a tri-linear material model, was used in a zero length rotational spring element to represent the response of the header plate connections. Tri-linear idealization of the moment-rotation connection response is developed as demonstrated in Fig. 5. As shown, the backbone response is constructed in such a way that the area A1 between the curve and tri-linear approximation is nearly equal to the area A2. Further, as shown in Fig. 5, which is plotted for only positive moments and rotations because of

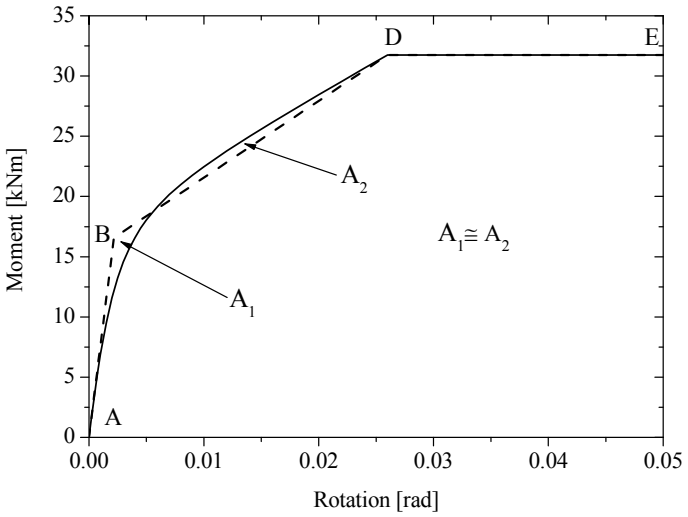

Fig. 5 Moment-rotation curve and idealization

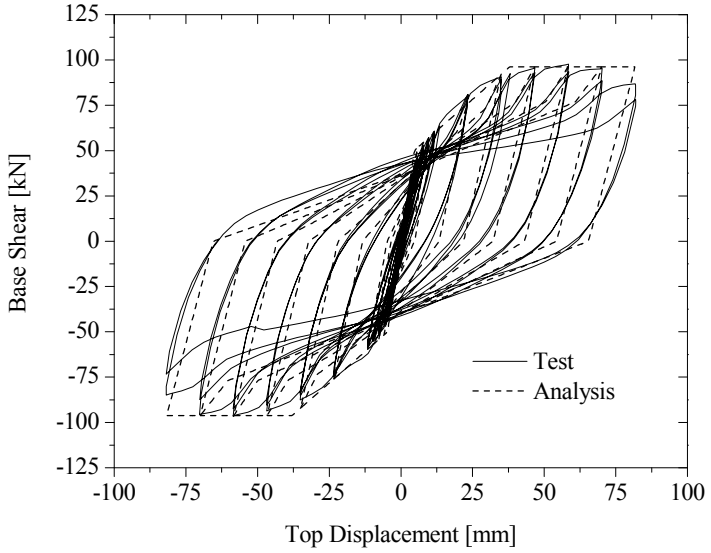

Fig. 6 Comparison between analytical and experimental hysteresis curves for BF-H specimen

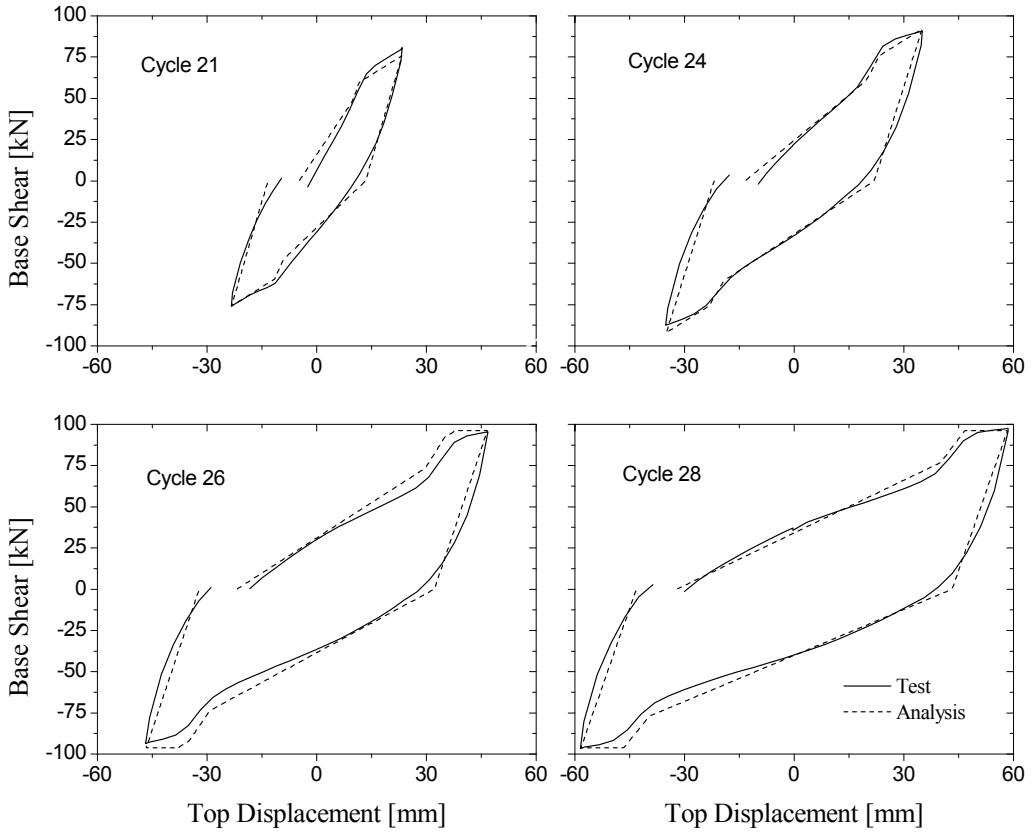

Fig. 7 Comparison between analytical and experimental hysteresis curves for the bare frame model

symmetry, it was assumed that moment capacity of the connection was achieved at a rotation of 0.026 rad, after which the moment-rotation curve was assumed to be flat. The adequacy of the moment-rotation curve for representing the header plate connection response was demonstrated by Vatansever and Yardımcı (2011).

An OpenSEES model of the bare frame was developed using the beam-to-column connection model described above and standard beam-column elements with elastic material properties for the frame members. This model was used to calibrate the cyclic hardening and pinching parameters necessary in the Hysteretic Material model used in the zero length rotational spring representing the connection against the bare frame experimental results. In the calibration of the cyclic parameters, the cycles after yielding were primarily considered due to their more significant contribution to the entire energy dissipation of the system. The Hysteretic Material parameters were adjusted such that the energy dissipation in a given cycle from the model was within 10% of the energy dissipation from the bare frame test. Figs. 6 and 7 show the resulting analytical bare-frame response and the experimental results for the entire loading duration (Fig. 6) and selected individual cycles (Fig. 7). Note that the loading protocol is discussed in Vatansever and Yardımcı (2011).

5. Analytical model for infill-to-boundary frame screwed connection

For TSPSWs with self-drilling screw connections there is considerable bearing deformation of the connections that must also be incorporated into the strip model for both monotonic and cyclic loading. It is apparent that screwed infill plate connections to the boundary frames significantly affect the general behavior of the specimens (Vatansever and Yardımcı 2011). Therefore, an analytical model is developed here based on the bearing deformations in the screw connections using experimental results from small component tests on such connections conducted by others. The models are then added to strip models of the TSPSWs described above to improve their representation of the cyclic behavior.

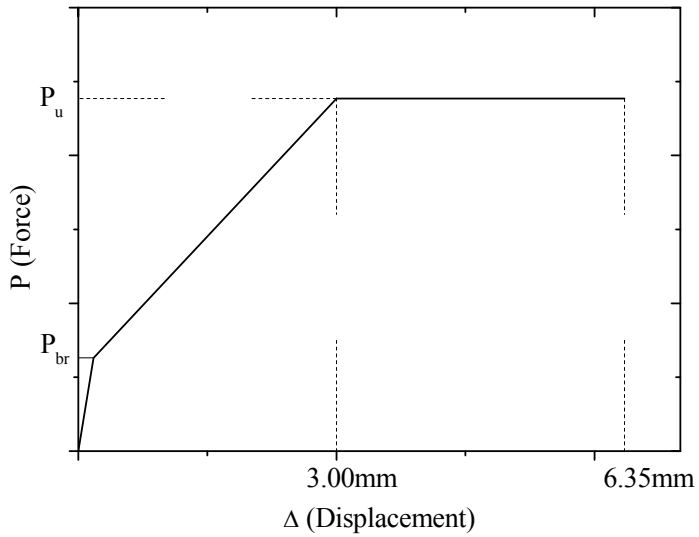

Fig. 8 Tri-linear curve bearing force-deformation relationship

In order to include the effects of the infill plate-to-boundary frame connection in the strip model of the TSPSWs the behavior of the screwed connection is studied in considerable detail. First, a single screw connection is analyzed using a detailed finite element model. The finite element modeling approach is first validated by applying it to model to a bolted connection and comparing the analysis results with available experimental results. Then, a relatively simple mechanics-based model developed by others to predict the bearing force versus bearing deformation behavior of bolted connections is modified for application to the screw connections considered here. Using the detailed finite element model, simple mechanics-based model, and ultimate strength equations from codes and the literature, a tri-linear curve bearing-force deformation relationship is established as shown in Fig. 8. The results of the FE analysis and mechanics-based analytical model will be used to establish the elastic and first yield behavior for the idealized tri-linear model and design code equations will be utilized to predict the ultimate strength for use in OpenSEES. For screw connections the ultimate bearing deformation of a single screw connection is given as 3.00 mm by ECCS TC7 (ECCS 2009). Here, this value of 3.00 mm is used for the upper bound of bearing deformation at the instant the ultimate strength of a single screw connection is attained. The ultimate bearing deformation is assumed to be 6.35 mm as recommended by Frank and Yura (1981).

5.1 Finite element model and validation

A detailed finite element (FE) model of a single screw connection was developed to provide additional confidence in approximating the behavior for OpenSEES. However, there is little test data available on the force-deformation behavior of screw connections, especially when screwed into a thicker backing plate like the fish plate in the TSPSWs. Therefore, a modeling method for the screw connections was developed by first modeling single bolt tests conducted by Rex and Easterling (2003). This approach is reasonable as long as the tilting deformation of the screw connection is negligible, which is the case in this application because of the thicker fish plate anchoring the screw and thinner infill plate at the screw head which will have considerable bearing deformations.

The finite element package ABAQUS (Hibbit et al. HKS) was used to model the bolted connection previously tested by Rex and Easterling (2003) which has single A325 bolt with the diameter of 25 mm. The plate width and thickness were 127 mm and 6.5 mm, respectively. The yield and ultimate strengths of the plate were given as 307 MPa and 452 MPa, respectively. The edge distance between the center of bolt hole and edge of the plate was taken as 38 mm. Two dimensional FE meshes using shell elements (ABAQUS element S4R), were used for developing the model. Shell elements were found to be capable of representing the load-deformation response of a single bolted connection by Kim and Kuwamura (2007). Contact between the screw body and screw hole was defined using surface-based contact option in ABAQUS. The load-deformation data from Rex and Easterling (2003) along with a plot of the FE results is presented in Fig. 9. From the figure, it can be seen that FE model reasonably approximates the test results.

The FE model of the single bolt connection was then extended to a single screw connection. As described above for the single bolt connection, shell elements (ABAQUS element S4R) were employed for the connecting plates and the screw body. Previous tests performed by Vatansever (2008) to establish the strength and failure mode of screw connections for TSPSWs revealed that failures normally do not take place in the screw itself as shown in Fig.10. In fact, in such tests with thin plates screwed to thicker fish plates there was very little evidence of screw deformation at all

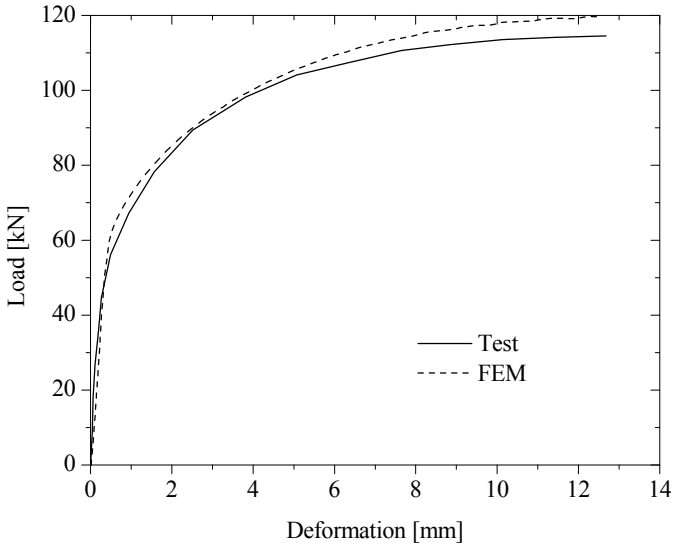

Fig. 9 Comparison between the load-deformation curves for FE model validation

Fig. 10 Failure modes of screw connections (Vatansever 2008)

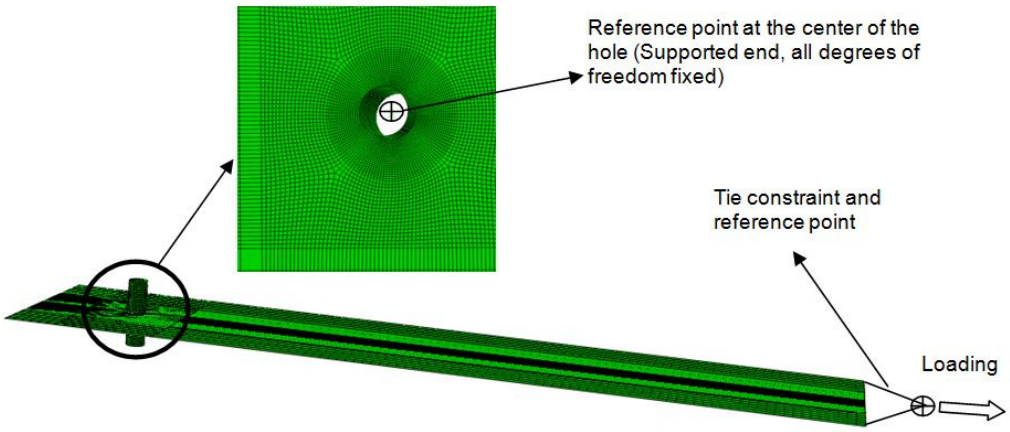

Fig. 11 Details of finite element model

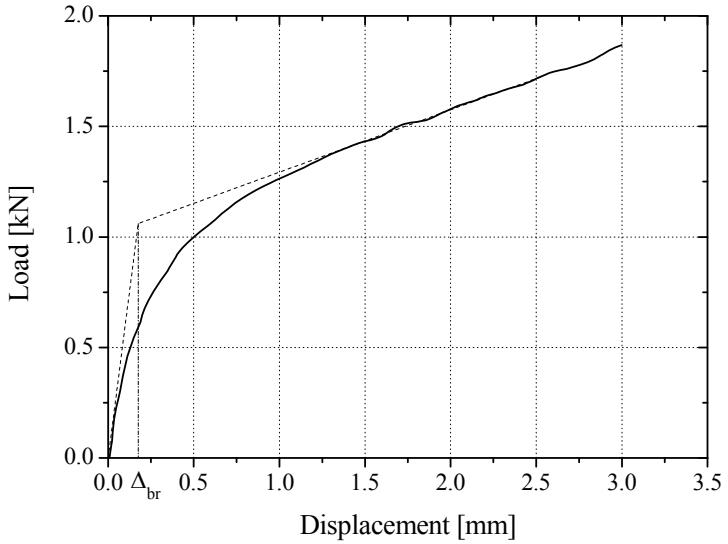

Fig. 12 Finite element analysis results of the single screw connection

prior to tear out from the thin plate. Therefore, it is assumed here that the screw has rigid body behavior in the connection assembly. Using the rigid body constraints the motion of the screw is constrained to the motion of the reference point defined at the center of the screw hole as shown in Fig. 11, which also shows the overall layout of the screw connection FE model.

The screw body was idealized such that it had the diameter of hole considered in the FE model. The screw size, plate thickness, and plate material were the same as those used in the TSPSW tests as described above. Boundary conditions were applied at both ends of the screw, where all degrees of freedom of the reference points at the center of each end of the screw hole were fixed. Because the connection assemblage typically has a washer underneath the screw head, out-of-plane deformations of the nodes around the screw hole were restrained. No friction between the screw surface and screw hole or screw head and plate was assumed. Loading was applied to the FE model as shown in Fig. 11 under displacement control where the prescribed displacement was imposed on a reference point defined at the end of the plate.

Fig. 12 shows the results of the FE analysis for a single screw connection with screw and plate properties equal to those from Specimen SW-A-H and the prediction of the characteristic value of Δ_{br} without screw thread depth. Only the displacements induced by the bearing deformations were considered in Fig. 12. The value of the Δ_{br}, which is estimated by considering the intersection point of the initial tangent and tangent in plastic region, is obtained as 0.175 mm for the Specimen SW-A-H. For the Specimen SW-B-H, this value is 0.165 mm.

5.2 Bearing force – deformation relationship

A bearing deformation model developed for bolted connections by Rex and Easterling (2003) is modified here for representing the behavior of screw connections connecting thin infill plates. This model is used to predict the connection force that corresponds to the bearing deformation of Δ_{br} as determined above. Fig. 13 shows the screw shank, screw hole and bearing deformation of the connecting infill plate. This figure is used to derive the load-deformation relationship between the

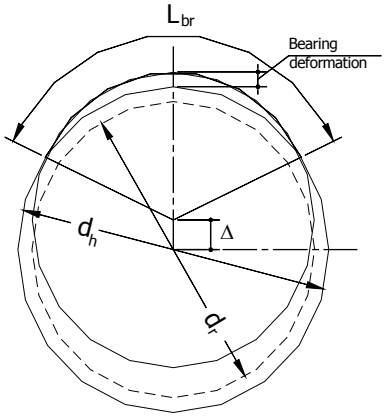

Fig. 13 Bearing deformation model (adapted from Rex and Easterling 2003)

hole and screw body. In this model, Δ is the total deformation, L_{br} is the bearing length around the perimeter of the hole, dh is the screw hole diameter which is assumed to be equal to the screw diameter with threads included, d_s, and d_r is the screw shank diameter. Assuming that once bearing occurs it occurs on the screw shaft rather than the threads, the bearing length can be calculated using the geometry of Fig. 13 as

$$L_{br} = \frac{\pi d_r}{2} - d_r \sin^{-1}\left(\frac{(d_h/2)^2 - (d_r/2)^2 - \Delta^2}{\Delta d_r}\right) \leq \frac{\pi d_r}{2} \tag{2}$$

where L_{br} is limited to half of the screw body perimeter because the contact perimeter between the screw body and hole cannot exceed half of the screw body perimeter. Note that the total displacement, Δ, is equal to the bearing deformation of Δ_{br} plus half of the difference between dh and d_r, which corresponds to the screw thread depth. Here, thread depth should be considered to avoid the numerical error in the implementation of the Eq. (2).

Note that the bearing length equation would be more complicated if the hole diameter were considered to be different from the screw diameter with threads. However, since screws are typically driven into place with no more than small pilot holes present, this assumption should be reasonable.

Using the bearing length, the connection force that corresponds to Δ can be found by using Eq. (3) as

$$P_{br} = L_{br} t F_u \tag{3}$$

where P_{br}, t and F_u are bearing force, infill plate thickness and tensile strength of infill material, respectively. For implementation of Eq. (2) the maximum total bearing deformation Δ is necessary and is taken as 3.00 mm at the instant the ultimate strength of a single screw connection is attained.

Fig. 14 shows the results of the FE analysis and the mechanics-based analytical model described above for a screw connection with screw and plate properties equal to those from Specimen SW-A-H. Note that the analytical model reaches a plateau when the bearing length, L_{br}, reaches half of the perimeter of the screw (i.e., the upper bound in Eq. (2)). As shown, both models

produce reasonably similar response to deformations of approximately 1.0 mm. Beyond that deformation, plate tearing is likely to begin and neither model is able to capture that behavior. Thus, for larger deformations the behavior will be approximated by design code values as described below.

Beyond the initial stiffness and onset of inelastic deformation predicted via the models above, the ultimate strength and deformation are also needed to complete the idealized tri-linear behavior shown in Fig. 15 for a single screw connection with the characteristics equal to those from Specimen SW-A-H.

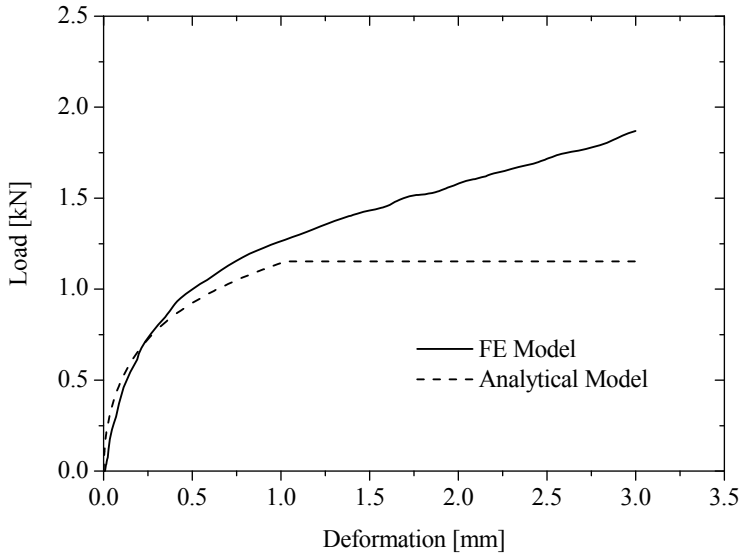

Fig. 14 Load-deformation curves for single screw connection

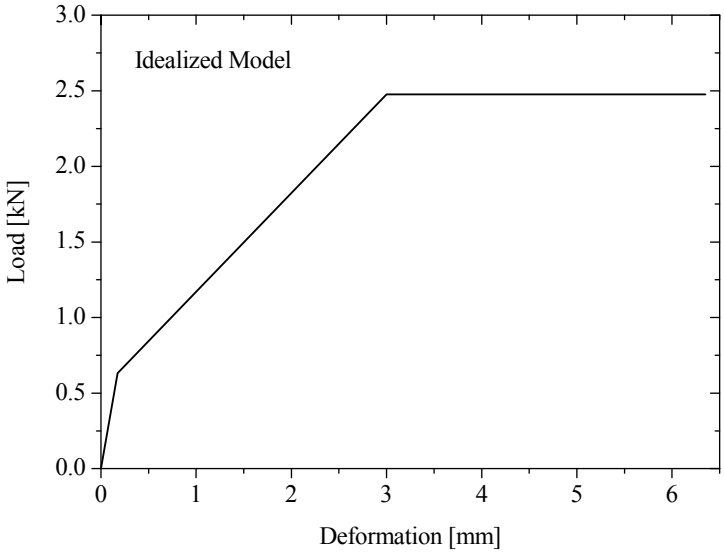

Fig. 15 Idealized load-deformation curve for single screw connection

As discussed above, the ultimate deformation is taken as 3.0 mm based on ECCS TC7 (ECCS 2009). The ultimate strength of a single screw connection, P_u, as given in Yu (2000) is used here

$$P_u = 2.7F_u t d_s \tag{4}$$

where d_s is the measured outside screw diameter. There are several equations for screw connection strength available in various international design codes. Eq. (4) was selected because it gave good agreement with the ultimate strengths of the single screw tests described in Vatansever (2008). The average ultimate strength from those tests, which used the same plate material and screws that were used in the TSPSW tests, was 2.45 kN while Eq. (4) predicted an ultimate strength of 2.39 kN.

5.3 Cyclic behavior models for screwed connections

Research by LaBoube and Sokol (2002) has demonstrated a group effect with screw connections such that the ultimate strength of a group of screw connections is somewhat less than the ultimate strength of a single screw connection as given by Eq. (4) times the number of screws. To account for this observation LaBoube and Sokol (2002) proposed a reduction factor, R, to modify the total strength of connections with multiple screws as a function of the number of screws, n. The reduction factor is given by

$$R = \left(0.535 + \frac{0.467}{\sqrt{n}} \right) \leq 1.0 \tag{5}$$

where n is the number of screws in the connection. It should be noted that LaBoube and Sokol (2002) recommended ranges for connection parameters for which this reduction factor was applicable based on the parameters of the connection that they had tested. For the TSPSW connections, some of the connection parameters (plate thickness and the ratio of the ultimate strength to yield strength of the plate) fall slightly outside the recommended ranges. However, because the values were close to the recommended ranges and little experimental data on connections configured like the TSPSW connections is available, Eq. (5) was employed for reducing the ultimate connection strength. Further, the observed group effect in screw connections was found to be independent of the screw layout, i.e., whether the screws were arranged parallel or perpendicular to the direction of the stress in the connecting plates (LaBoube and Sokol 2002). Thus the reduction factor is applicable to the connection configuration considered here making the yield $P_{br,conn}$ and ultimate screw connection strength, $P_{u,conn}$

$$P_{br,conn} = RnL_{br}tF_u \tag{6}$$

$$P_{u,conn} = 2.7RnF_u t d_s \tag{7}$$

Hence, the yield strength and the ultimate capacity of each strip connection to the boundary frame can be computed by using Eqs. (6) and (7), respectively.

The tests conducted by LaBoube and Sokol (2002) considered connections with only up to 8 screws and the tests indicated that the strength reduction was reaching a plateau. Thus instead of considering a strength reduction here based on the entire infill plate-to-boundary frame connection, a reduction was applied based on the number of screws per strip in the strip model representation

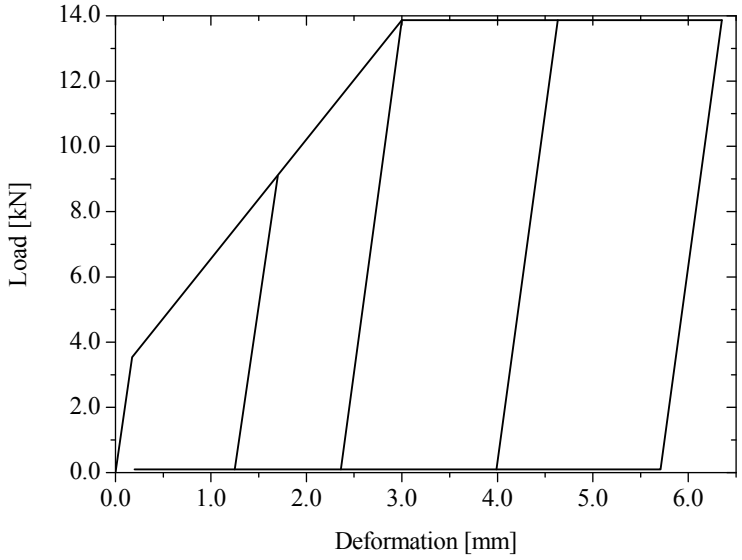

Fig. 16 Cyclic behavior model of screwed connection of SW-A-H

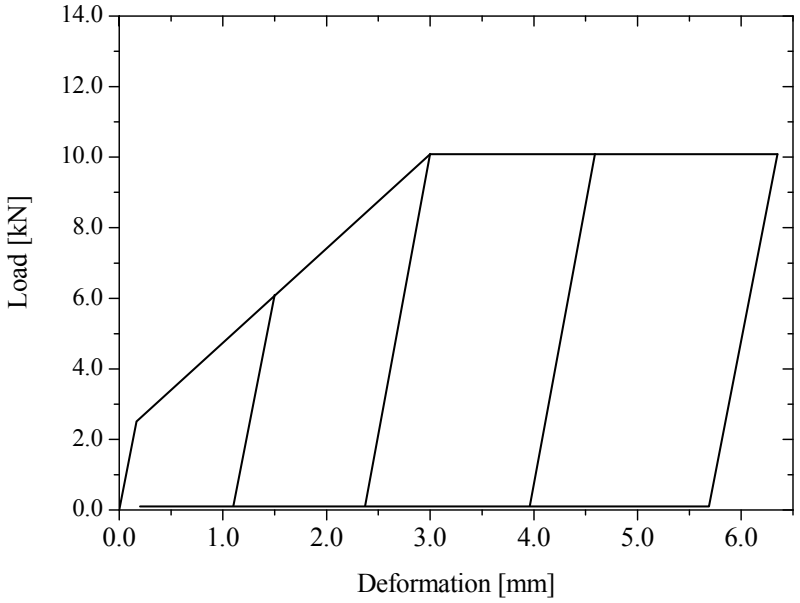

Fig. 17 Cyclic behavior model of screwed connection of SW-B-H

of the infill plate. It was determined from the infill plate connection geometry and the development of the strip models of the specimens as described below that on average there were 8 and 6 screws per strip for Specimens SW-A-H and SW-B-H, respectively. Therefore, given the infill plate thickness, yield strength, and number of screws per strip, the tri-linear curve used for modeling the screw connection at each end of the each strip in the strip models is given in Figs. 16 and 17. Those figures also show the assumed unloading response for cyclic loading. Note that since the

strips are tension only, as described further below, the screw connection models are not subjected to compressive loads. The next section describes the implementation of this screw connection representation in the strip models of the TSPSW specimens.

6. Modeling of the specimens

The structural analysis software OpenSEES (Mazzoni *et al*. 2009) was employed in the modeling of the TSPSW specimens using the strip model method. These models can be used to facilitate a comparison with experimental results, and to explore the use of the strip model for representing infill plates that are connected to the boundary frames via screws. Gravity load was not applied in the testing or in the models.

All models were pinned at the column bases to replicate the test conditions. Out-of-plane displacements of the specimens were restrained at the upper beam. As described above, the infill plates were represented by a series of discrete, pin-ended strips inclined in the direction of the tension field using truss elements. Figs. 18 and 19 show the layouts of the strip models of Specimens SW-A-H and SW-B-H, respectively. The typical cyclic tension only behavior of a strip is shown in Fig. 20.

In all models, nonlinear beam-column elements were used for boundary frame members. The screw connections were modeled with zero-length elements at the end of each strip and given the axial force- deformation behavior shown in Figs. 16 and 17. The axes of the zero-length elements were rotated by the inclination angle of the strips. Beam-to-column connections were modeled

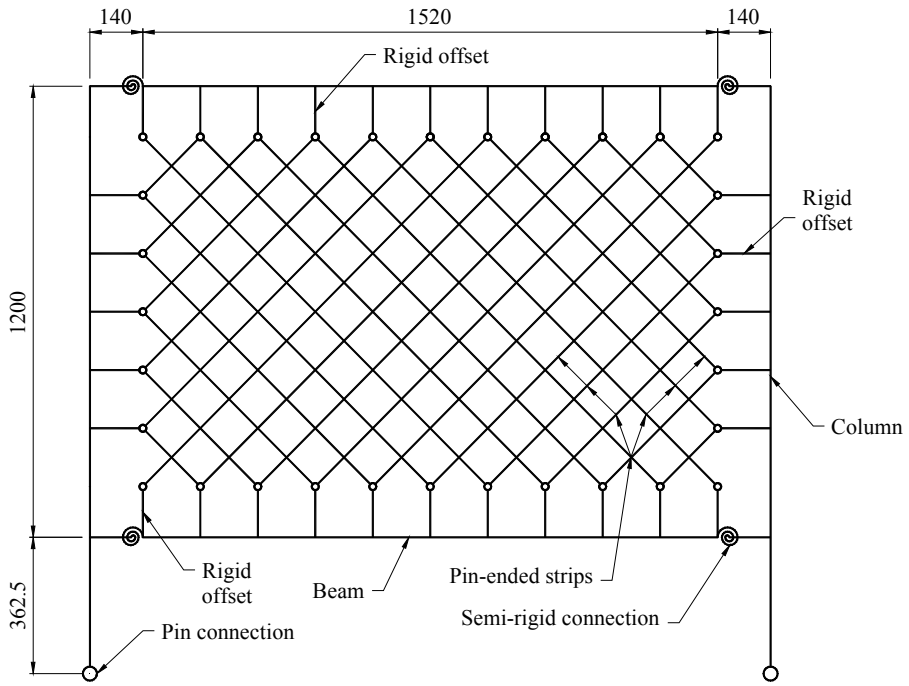

Fig. 18 OpenSEES model of Specimen SW-A-H (Dimensions in mm)

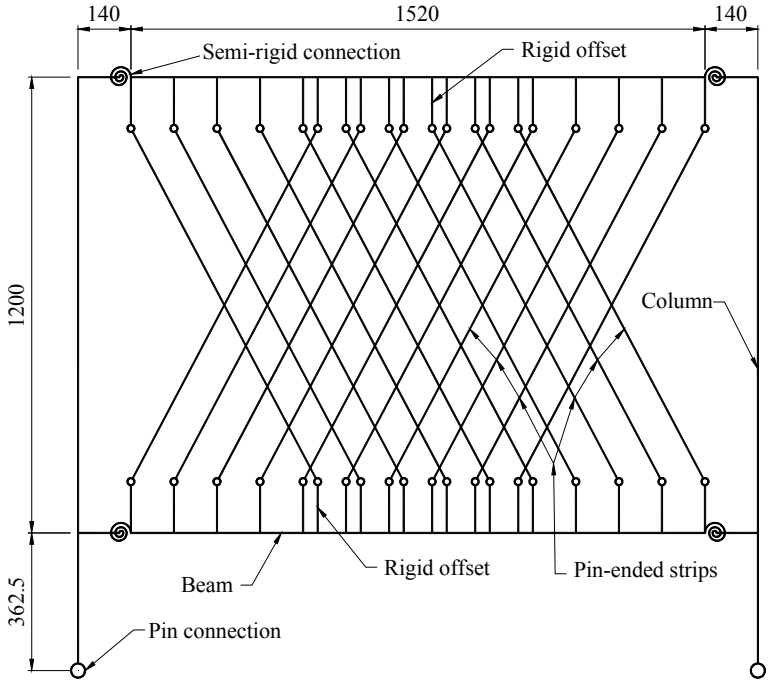

Fig. 19 OpenSEES model of Specimen SW-B-H (Dimensions in mm)

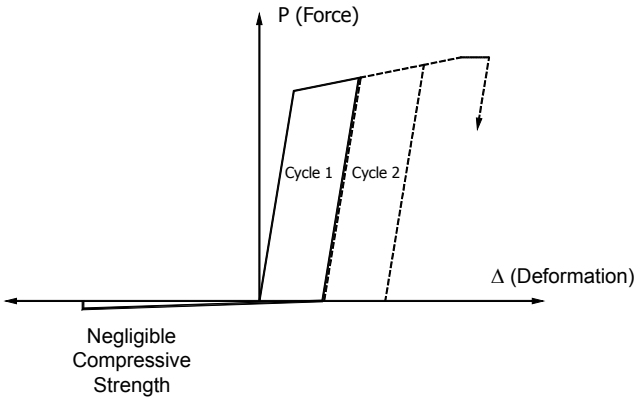

Fig. 20 Cyclic axial load behavior of a strip

using zero-length elements with the moment-rotation behavior described above that represents the header plate connection response. The elements were placed at the location of the column flange and rigid offsets were used to connect to the nonlinear beam-column element at the column centerline. For all zero length elements, only the degrees of freedom where nonlinear properties were applied were free to move (axis 1 for the screw connection elements and rotation about the z axis for beam-to-column connection elements) while all other degrees of freedom were constrained.

The inclination angle of the strips for SW-A-H is computed through consideration of Eq. (8)

(Timler and Kulak 1983), resulting in 44.3°. For the orientation of the strips in SW-B-H, the incomplete diagonal tension field theory was considered (Thorburn *et al*. 1983), where the inclination angle of the tension field, α, is equal to $tan^{-1}(L/h)$ / 2, resulting in 28.2° with respect to vertical.

$$tan^4 \alpha = \frac{1 \times \frac{tL}{2A_c}}{1 + th\left(\frac{1}{A_b} + \frac{h^3}{360 I_c L}\right)} \tag{8}$$

α is the inclination angle of a strip
t is the thickness of the infill plate
L is the width of the SPSW (between column centerlines)
A_c is the section area of the column
h is the height of the SPSW (between beam centerlines)
A_b the section area of the beam
I_c is the inertia moment of the column

In order to account for the eccentricity between the infill plate edges and centerlines of the boundary frame members, rigid offsets whose length were half of the section depths of the boundary frame members were utilized. Tension test results for yield stress and elastic modulus from the material test data for the infill plates described above were used for the material properties of the strip elements. The yield stress and elastic modulus of the boundary frame members was taken to be 275 MPa and 210000 MPa, respectively in the absence of coupon test results. Fish plates were not represented in the models because their effects were found to be negligible (Driver *et al*. 1998a).

7. Comparison and discussion

The analytical hysteresis curves using the strip models including the screw connection behavior are compared with the experimental results for Specimens SW-A-H and SW-B-H in Figs. 21 and 22, respectively. The comparison indicates that the analytical model including screw connection behavior model predicts the test results reasonably well. In particular, the initial stiffness, post-yield stiffness and unloading stiffness of the specimens are well represented considering the complexity of the behavior of the TSPSWs. In order to show the contribution of the screw connection model to the overall behavior of the analytical models, the hysteretic loops of the SW-A-H and SW-B-H without the screw connection behavior model were also superimposed on each test result in Figs. 21 and 22, respectively. As the figures show, the screw connection model is necessary to accurately represent the systems' initial stiffness but does not significantly impact the models' estimation of the specimens' strength.

As shown in Fig. 24, the yield force for Specimen SW-B-H is somewhat underestimated by the strip model with the screw connection model. There are several possible reasons for this including: (i) the reduction factor for the screw connection models may be too large; (ii) the incomplete tension field inclination angle may not properly represent the orientation of the tension field when the infill plate is connected only to the beams; or (iii) more screws were activated for loading in each than assumed by using those tributary to each strip. Note that because the screw connection

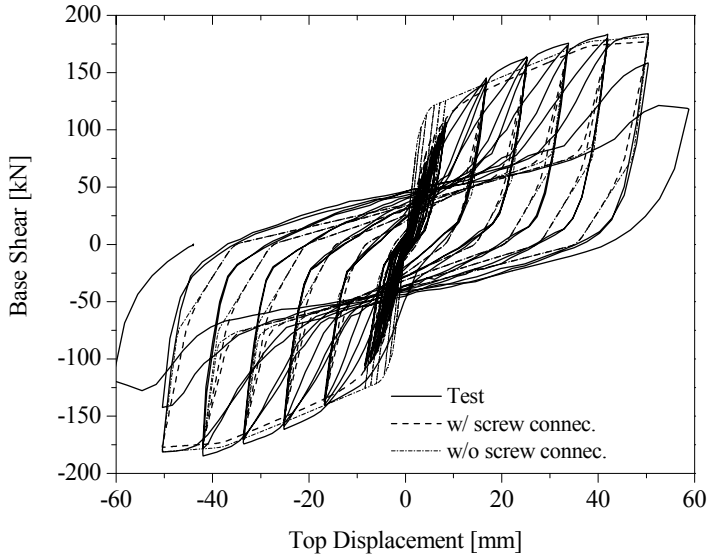

Fig. 21 Comparison between analytical and experimental hysteresis curves for SW-A-H specimen

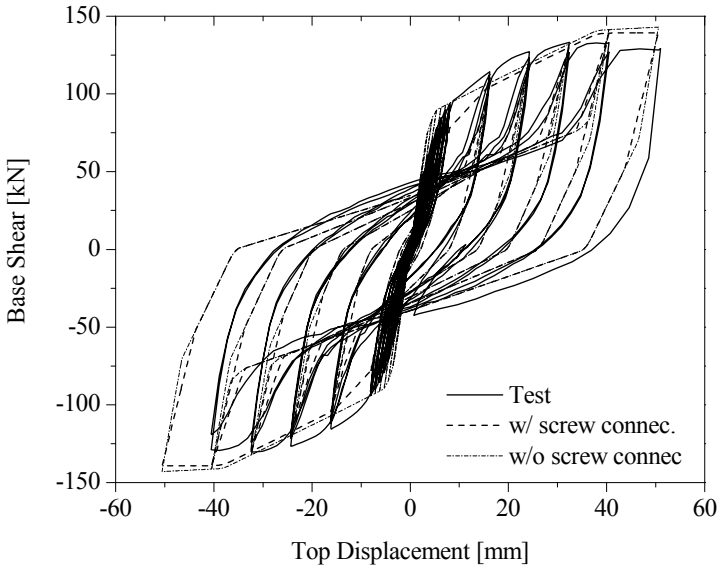

Fig. 22 Comparison between analytical and experimental hysteresis curves for SW-B-H specimen

behavior for each strip considered the average number of screws tributary to each strip, for Specimen SW-B-H this means that there were a number of screws that were not assumed to participate in the loading in one particular direction. Despite these differences, the simple screw connection model proposed was able to represent the cyclic inelastic response of the TSPSW specimen with reasonable accuracy.

In general, the bearing deformations that occurred at the infill plate-to-fish plate screw connections caused the initial stiffness of the systems to be decreased relative to TSPSWs having a

more rigid connection. This also increases the deformation at which yielding takes place. However, the tests showed that a simple and easy to install screw connection can develop full tension field yielding of the infill plates and a very ductile response. Further, the analysis approach developed here can be used for design and evaluation of this promising lateral load resisting system.

8. Conclusions

Two TSPSW specimens with self-drilling screw infill plate-to-boundary frame connections were tested and exhibited ductile response. A bare frame identical to the boundary frame in the TSPSW specimens was also tested and used to calibrate a moment-rotation model for the beam-to-column connections. Conventional TSPSW strip models were developed and it was shown that the behavior of the screw connections contributed significantly to the response, requiring the development of a numerical model to represent the screw connections that could be implemented within the TSPSW strip models. A mechanics-based model and more detailed FE model were both developed to provide an estimation of the initial stiffness of the screw connection. Similar results were obtained for each and the mechanics-based model was combined with building code equations for ultimate screw strength and maximum connection deformation to establish a tri-linear force-displacement curve representative of screw connections.

The screw model was implemented in strip models of the TSPSW test specimens and good agreement was obtained in terms of stiffness and overall hysteretic behavior. Modeling was found to more accurately represent the behavior of the specimen having its infill plate connected to the boundary frame around its entire perimeter while it underestimated the yield base shear for the specimen with infill connections to only the boundary frame beams. The general formulation of the strip model, screw connection model, and beam-to-column connection model should enable others to adequately analyze similar systems under large seismic demands in nonlinear analysis. Additional research is still necessary on the bearing deformation characteristics for the screw connections with parameters beyond those tested here and on the general behavior of TSPSW systems having infill plates connected only to the boundary frame beams.

References

Abbott, B.J. and Richard, R.M. (1975), "Versatile elastic-plastic stress-strain formula", *J. Eng. Mech. Div.*, **101**(4), 511-515.

Applied Technology Council (ATC) (1992), ATC-24 Guidelines for Cyclic Seismic Testing of Components of Steel Structures, CA, USA.

Berman, J. and Bruneau, M. (2005), "Experimental investigation of light-gauge steel plate shear walls", *J. Struct. Eng.*, **131**(2), 259-267.

Caccese, V., Elgaaly, M. and Chen, R. (1993), "Experimental study of thin steel-plate shear walls under cyclic loading", *J. Struct. Eng.*, **119**(2), 0573-0587.

Chen, S.J. and Jhang, C. (2006), "Cyclic behavior of low yield point steel shear walls", *Thin-Wall. Struct.*, **44**(2006), 730-738.

Choi, I.R. and Park, H.G. (2009), "Steel plate shear walls with various infill plate designs", *J. Struct. Eng.*, **135** (7), 785-796.

Driver, R.G., Kulak, G.L., Elwi, A.E. and Kennedy, D.J.L. (1998a), "FE and simplified models of steel plate shear wall", *J. Struct. Eng.*, **124**(2), 0121-0130.

Driver, R.G., Kulak, G.L., Kennedy, D.J.L. and Elwi, A.E. (1998b), "Cyclic test of four-story steel plate shear wall", *J. Struct. Eng.*, **124**(2), 0112-0120.

Elgaaly, M. and Liu, Y. (1997), "Analysis of thin-steel-plate shear walls", *J. Struct. Eng.*, **123**(11), 1487-

1496.
European Convention for Constructional Steelwork (ECCS), ECCS-TC7 (2009), The Design and Testing of Connections in Steel Sheeting and Sections, 124.
European Convention for Constructional Steelwork (ECCS) (2005), Eurocode 3; Design of Steel Structures, CEN, Brussels, Belgium.
Frank, K.H. and Yura, J.A. (1981), "An experimental study of bolted shear connections", Technical Report No. FHWA/RD-81/148; Department of Civil Engineering, University of Texas at Austin, Austin, TX, USA.
Goldberg, J.E. and Richard, R.M. (1963), "Analysis of nonlinear structures", *J. Struct. Div.*, **89**(4), 333-351.
Guo, L., Li, R., Rong, Q. and Zhang, S. (2012), "Cyclic behavior of SPSW and CSPSW in composite frame", *Thin-Wall. Struct.*, **51**(2012), 39-52.
Hibbit, Karlsson, Sorenson, Inc. (HKS), ABAQUS/Standard Theory Manual.
Jahanpour, A., Moharrami, H. and Aghakoochak, A. (2011), "Evaluation of ultimate capacity of semi-supported steel shear walls", *J. Construct. Steel Res.*, **67**(2011), 1022-1030.
Jahanpour, A., Jönsson, J. and Moharrami, H. (2012), "Seismic behavior of semi-supported steel shear walls", *J. Construct. Steel Res.*, **74**(2012), 118-133.
Kharrazi, M.H.K., Prion, H.G.L. and Ventura, C.E. (2008), "Implementation of M-PFI method in design of steel plate shear walls", *J. Construct. Steel Res.*, **64**(2008), 465-479.
Kharrazi, M.H.K., Ventura, C.E. and Prion, H.G.L. (2011), "Analysis and design of steel plate walls: Analytical model", *Can. J. Civ. Eng.*, **38**, 49-59.
Kim, T.S. and Kuwamura, H. (2007), "Finite element modeling of bolted connections in thin-walled stainless steel plates under static shear", *Thin-Wall. Struct.*, **45**(2007), 407-421.
Kurata, M., Leon, R.T., DesRoches, R. and Nakashima, M. (2012), "Steel plate shear wall with tension-bracing for seismic rehabilitation of steel frames", *J. Construct. Steel Res.*, **71**(2012), 92-103.
LaBoube, R.A. and Sokol, M.A. (2002), "Behavior of screw connections in residential construction", *J. Struct. Eng.*, **128**(1), 115-118.
Lubell, A.S., Prion, H.G.L., Ventura, C.E. and Rezai, M. (2000), "Unstiffened steel plate shear wall performance under cyclic loading", *J. Struct. Eng.*, **126**(4), 0453-0460.
Matteis, G.D. and Landolfo, R. (1999), "Mechanical fasteners for cladding sandwich panels: Interpretative models for shear behavior", *Thin-Wall. Struct.*, **35**(1999), 61-79.
Mazzoni, S., McKenna, F., Scott, M.H., Fenves, G.L. (2009), OpenSEES (Open System for Earthquake Engineering Simulation), Pacific Earthquake Engineering Research Center, University of California, Berkeley.
Rex, C.O. and Easterling, S.W. (2003), "Behavior and modeling of a bolt bearing on a single plate", *J. Struct. Eng.*, **129**(6), 792-800.
Sabelli, R. and Bruneau, M. (2007), Design Guide 20 Steel Plate Shear Walls; American Institute of Steel Construction.
Sabouri-Ghomi, S., Ventura, C.E. and Kharrazi, M.H.K. (2005), "Shear analysis and design of ductile steel plate shear walls", *J. Struct. Eng.*, **131**(6), 878-889.
Thorburn, L.J., Kulak, G.L. and Montgomery, C.J. (1983), "Analysis of Steel Plate Shear Walls", Structural Engineering Report No. 107; Department of Civil Engineering, University of Alberta, Edmonton, AB, USA.
Timler, P.A. and KuIak, G.L. (1983), "Experimental Study of Steel Plate Shear Walls", Structural Engineering Report No. 114; Department of Civil Engineering, University of Alberta, Edmonton, AB, USA.
Vatansever, C. (2008), "Cyclic Behavior of Thin Steel Plate Shear Walls with Semi-Rigid Beam-to-Column Connections", Ph.D. Thesis; Istanbul Technical University, Institute of Science.
Vatansever, C. and Yardımcı, N. (2011), "Experimental investigation of thin steel plate shear walls with different infill-to-boundary frame connection", *Steel Comp. Struct., Int. J.*, **11**(3), 251-271.
Yu, W.W. (2000), *Cold-Formed Steel Design*, John Wiley & Sons, Inc., New York, NY, USA.

CC